15 Electron-Phonon Coupling

Rolf Heid
Institute for Solid State Physics
Karlsruhe Institute of Technology

Contents

E. Pavarini, E. Koch, R. Scalettar, and R. Martin (eds.)
The Physics of Correlated Insulators, Metals, and Superconductors
Modeling and Simulation Vol. 7
Forschungszentrum Jülich, 2017, ISBN 978-3-95806-224-5
http://www.cond-mat.de/events/correl17

1 Introduction

The electron-phonon interaction is, besides the Coulomb interaction, one of the fundamental interactions of quasiparticles in solids. It plays an important role for a variety of physical phenomena. In particular in metals, low-energy electronic excitations are strongly modified by the coupling to lattice vibrations, which influences, e.g., their transport and thermodynamic properties. Electron-phonon coupling (EPC) also provides in a fundamental way an attractive electron-electron interaction, which is always present and, in many metals, is the origin of the electron pairing underlying the macroscopic quantum phenomenon of superconductivity.
This lecture addresses the consequences of electron-phonon coupling in both the normal and the superconducting state of metals. In Section 2, the basic Hamiltonian describing the coupled electron-phonon system is introduced. In Section 3, a closer look onto normal state effects in a metal is taken, focusing on the renormalization of quasiparticles, which allows to experimentally quantify the strength of the interaction. Section 4 is devoted to phonon-mediated superconductivity. First a derivation of the effective attractive interaction among electrons mediated by phonon exchange is given. Then we analyze the role of electron-phonon coupling for superconductivity in the context of the strong-coupling Migdal-Eliashberg theory in some detail. In Section 5, we discuss the density-functional based technique to calculate electron-phonon coupling quantities and present two examples to illustrate its predictive power. Throughout this Chapter, only nonmagnetic states are considered and atomic units $\hbar = 2m_e = e^2/2 = 1$ as well as $k_B = 1$ are used.

2 Electron-phonon Hamiltonian

2.1 Electron-phonon vertex

The lowest-order process involving the electron-phonon interaction is the scattering of a single electron by a simultaneous creation or annihilation of a single phonon, as diagrammatically shown in Fig. 1. The probability for the scattering process is called the electron-phonon vertex g. We will briefly sketch its derivation starting from rather general grounds. For more details one can refer to the book of Grimvall [1].
Due to the large ratio of the ionic and electronic mass, the dynamics of the ions and the electrons can be systematically expanded in terms of the small parameter $\kappa = (m/M)^{1/4}$, which results in a partial decoupling [2, 3]. To lowest order in κ, called the adiabatic or Born-Oppenheimer approximation, the total wavefunction of the coupled electron-ion system can be written as a product $\Psi(\underline{\mathbf{r}}, \underline{\mathbf{R}}) = \chi(\underline{\mathbf{R}})\psi(\underline{\mathbf{r}}; \underline{\mathbf{R}})$, where $\underline{\mathbf{r}}$ and $\underline{\mathbf{R}}$ denote the sets of electron and ion coordinates, respectively. The electronic wavefunction obeys the equation

$$[T_e + V_{ee} + H_{e-i}(\underline{\mathbf{R}})]\psi_n(\underline{\mathbf{r}}; \underline{\mathbf{R}}) = E_n(\underline{\mathbf{R}})\psi_n(\underline{\mathbf{r}}; \underline{\mathbf{R}})\,, \tag{1}$$

where T_e and V_{ee} denote the kinetic energy and Coulomb interaction of the electron system, respectively. Eq. (1) depends parametrically on the ionic positions $\underline{\mathbf{R}}$ via the electron-ion interaction H_{e-i}.

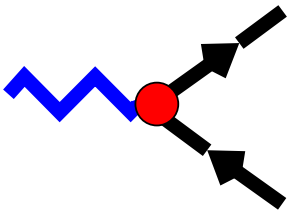

Fig. 1: *Diagrammatic representation of the basic electron-phonon scattering process. Black lines represent electrons, the blue zigzag line a phonon, and the red circle the screened vertex.*

The electron-phonon vertex appears in first order beyond the adiabatic approximation. One can show that it induces off-diagonal matrix elements among the electronic eigenstates ψ_n and has the form

$$\langle n|\delta_{\mathbf{R}} V|n'\rangle \,. \tag{2}$$

The operator $\delta_{\mathbf{R}} V$ stands for the linear change of the potential felt by the electrons under a displacement of an atom from its rest position: $\mathbf{R} = \mathbf{R}_0 + \mathbf{u}$. If the potential V is the bare electron-ion potential V^0, then $\delta_{\mathbf{R}} V = \mathbf{u} \cdot \nabla V^0|_{\mathbf{R}_0}$. Eq. (2) represents the bare vertex. However, in solids, and in particular in metals, the bare electron-ion potential is screened by the other electrons. Screening also alters the vertex significantly. Within linear response theory this operator takes the form

$$\delta_{\mathbf{R}} V = \mathbf{u} \cdot \epsilon^{-1} \nabla V^0|_{\mathbf{R}_0} \,, \tag{3}$$

where ϵ^{-1} is the inverse dielectric matrix [4], which is a measure of the screening. Note that in Eq. (3), the screening operator does not commute with the gradient operation, and thus can not be written in terms of the gradient of a screened potential.

2.2 Fröhlich Hamiltonian

We now aim to develop a systematic perturbative treatment of the mutual influence of the electronic and phononic subsystems in a solid. Thereby the question arises, what are the proper noninteracting quasiparticles to start with. The correct answer requires to know the solution to some extent. As we will see, electronic states are significantly influenced by lattice vibrations mostly in close vicinity of the Fermi energy. It is therefore appropriate to start with electrons moving in the static potential of a rigid ion lattice, without any renormalization by the lattice vibrations. On contrast, the bare vibrations of the ion lattice would be a bad starting point, because they are strongly altered by the screening of the electrons. This screening must be built into the description of the harmonic lattice vibrations which defines the noninteracting phonons. For the discussion of electron-phonon coupling effects in periodic solids, a good starting point is the *Fröhlich Hamiltonian*, which reads in second quantization

$$H = H_e + H_{ph} + H_{e-ph} \,. \tag{4}$$

Here the electron system is described by noninteracting quasi-particles with dispersion ε_k. These quasiparticles are considered to be the stationary solutions of band electrons in a perfect periodic lattice, and include already the renormalization from Coulomb interaction

$$H_e = \sum_{\mathbf{k}\nu\sigma} \varepsilon_{\mathbf{k}\nu}\, c^\dagger_{\mathbf{k}\nu\sigma} c_{\mathbf{k}\nu\sigma}\,. \tag{5}$$

Here $c_{\mathbf{k}\nu\sigma}$ ($c^\dagger_{\mathbf{k}\nu\sigma}$) are the annihilation (creation) operators for an electronic state with momentum $\mathbf{k}$, band index ν, spin σ, and band energy $\varepsilon_{\mathbf{k}\nu}$.
The lattice Hamiltonian is expressed in terms of quantized harmonic vibrations, and represents noninteracting phonons

$$H_{ph} = \sum_{\mathbf{q}j} \omega_{\mathbf{q}j} \left(b^\dagger_{\mathbf{q}j} b_{\mathbf{q}j} + \frac{1}{2} \right), \tag{6}$$

where $b_{\mathbf{q}j}$ ($b^\dagger_{\mathbf{q}j}$) are the annihilation (creation) operators for a phonon with momentum $\mathbf{q}$, branch index j, and energy $\omega_{\mathbf{q}j}$. Phonons are the quanta of the normal mode vibrations (for more details see Appendix A). The operator of atom displacements is expressed in terms of the phonon operators by

$$u_{ls\alpha} = e^{i\mathbf{q}\mathbf{R}^0_{ls}} \frac{1}{\sqrt{N_q}} \sum_{\mathbf{q}j} A^{\mathbf{q}j}_{s\alpha} \left(b_{\mathbf{q}j} + b^\dagger_{-\mathbf{q}j} \right) \qquad \text{with} \qquad A^{\mathbf{q}j}_{s\alpha} = \frac{\eta_{s\alpha}(\mathbf{q}j)}{\sqrt{2M_s\omega_{\mathbf{q}j}}}\,. \tag{7}$$

Atoms are characterized by two indices denoting the unit cell (l) and the atoms inside a unit cell (s), respectively, with M_s the corresponding atom mass. α denotes Cartesian indices, and $\eta_{s\alpha}(\mathbf{q}j)$ is the eigenvector of the normal mode $\mathbf{q}j$. The number of points in the summation over $\mathbf{q}$ is N_q.
The third term describes the lowest-order coupling between electrons and phonons derived from Eq. (3). Using the relationship Eq. (7) it has the form

$$H_{e-ph} = \sum_{\mathbf{k}\nu\nu'\sigma} \sum_{\mathbf{q}j} g^{\mathbf{q}j}_{\mathbf{k}+\mathbf{q}\nu',\mathbf{k}\nu} c^\dagger_{\mathbf{k}+\mathbf{q}\nu'\sigma} c_{\mathbf{k}\nu\sigma} \left(b_{\mathbf{q}j} + b^\dagger_{-\mathbf{q}j} \right)\,. \tag{8}$$

$g^{\mathbf{q}j}_{\mathbf{k}+\mathbf{q}\nu',\mathbf{k}\nu}$ is the electron-phonon matrix element and describes the probability amplitude for scattering an electron with momentum $\mathbf{k}$ from band ν to a state with momentum $\mathbf{k}+\mathbf{q}$ in band ν' under the simultaneous absorption (emission) of a phonon with momentum $\mathbf{q}$ ($-\mathbf{q}$) and branch index j

$$g^{\mathbf{q}j}_{\mathbf{k}+\mathbf{q}\nu',\mathbf{k}\nu} = \sum_{s\alpha} A^{\mathbf{q}j}_{s\alpha} \langle \mathbf{k}+\mathbf{q}\nu'\sigma | \delta^{\mathbf{q}}_{s\alpha} V | \mathbf{k}\nu\sigma \rangle\,. \tag{9}$$

Here again the screened first-order variation enters the matrix elements. They are independent of spin for nonmagnetic ground states.
This general form of the Fröhlich Hamiltonian will be the starting point for the many-body perturbation outlined in the next Sections. To simplify the treatment, we will use a compact notation combining momentum and band/branch index into a single symbol: $k = (\mathbf{k}\nu)$, $k' = (\mathbf{k}'\nu')$, and $q = (\mathbf{q}j)$. The EPC matrix elements are then denoted as

$$g^q_{k',k} = g^{\mathbf{q}j}_{\mathbf{k}'\nu',\mathbf{k}\nu} \delta_{\mathbf{k}',\mathbf{k}+\mathbf{q}}\,, \tag{10}$$

which implicitly takes into account momentum conservation.

3 Normal-state effects

3.1 Green functions and perturbation

In this section we will discuss the effects of electron-phonon interaction in the normal state of a metal. This will be done using many-body perturbation techniques [5–7]. The focus will be on the renormalization of electronic and phononic quasiparticles, which provides ways to experimentally gain information about the coupling strength. This will set the stage for the discussion of phonon-mediated superconductivity in the next section.

The following treatment is based on the Fröhlich Hamiltonian Eq. (4), where $H_0 = H_e + H_{ph}$ denotes the Hamiltonian of the unperturbed quasiparticles and H_{e-ph} is perturbation linear in the electron-phonon coupling. We will work with the imaginary-time Green functions

$$G(k,\tau) = -\langle T_\tau c_{k\sigma}(\tau) c^\dagger_{k\sigma}(0)\rangle \tag{11}$$

for the fermionic quasiparticles, where the field operators are given in a Heisenberg picture using an imaginary time $-i\tau$, $c_{k\sigma}(\tau) = e^{H\tau} c_{k\sigma} e^{-H\tau}$ with $-\beta < \tau < \beta$, $\beta = 1/T$. The Wick operator T_τ reorders operators to increasing τ from right to left.

For the bosonic quasiparticles, the Green function of the displacement operators is defined as

$$U_{s\alpha,s'\alpha'}(\mathbf{q},\tau) = -\langle T_\tau u_{\mathbf{q}s\alpha}(\tau) u_{-\mathbf{q}s'\alpha'}(0)\rangle = \sum_j A^{\mathbf{q}j}_{s\alpha} A^{-\mathbf{q}j}_{s'\alpha'} D(\mathbf{q}j,\tau)\,, \tag{12}$$

where D denotes the phonon Green function ($q = (\mathbf{q}j)$)

$$D(q,\tau) = -\langle T_\tau (b_q(\tau) + b^\dagger_{-q}(\tau))(b_{-q}(0) + b^\dagger_q(0))\rangle \tag{13}$$

$G(k,\tau)$ and $D(q,\tau)$ can be defined as periodic functions in τ with symmetry properties $G(k,\tau+\beta) = -G(k,\tau)$ and $D(k,\tau+\beta) = D(k,\tau)$, respectively. Their Fourier transforms are given by

$$G(k,i\omega_n) = \frac{1}{2}\int_{-\beta}^{\beta} d\tau\, e^{i\omega_n\tau} G(k,\tau) \tag{14}$$

$$D(q,i\nu_m) = \frac{1}{2}\int_{-\beta}^{\beta} d\tau\, e^{i\nu_m\tau} D(q,\tau)\,, \tag{15}$$

where $\omega_n = (2n+1)\pi T$ and $\nu_m = 2m\pi T$, with n, m integer values, denote fermionic and bosonic Matsubara frequencies, respectively.

Two further simplifications have been assumed: (i) because we are dealing with nonmagnetic states only, the spin index in the electronic Green function can be suppressed; (ii) the perturbation H_{e-ph} does not mix different electronic bands or phononic modes, such that the interacting Green functions can still be represented by a single band/mode index.

The bare Green functions of the unperturbed Hamiltonian $H_0 = H_e + H_{ph}$ are

$$G_0(k,i\omega_n) = \frac{1}{i\omega_n - \varepsilon_k} \tag{16}$$

$$D_0(q,i\nu_m) = \frac{1}{i\nu_m - \omega_q} - \frac{1}{i\nu_m + \omega_q}\,. \tag{17}$$

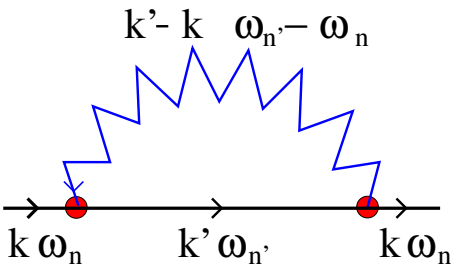

Fig. 2: *Diagrammatic representation of the lowest-order contribution to the electron self-energy from the electron-phonon coupling. Blue zigzag and black lines represent phonon and electron propagators, respectively.*

Electronic energies are measured with respect to the chemical potential. By applying many-body perturbation theory to the Fröhlich Hamiltonian, the interacting Green functions are expressed by an infinite series of Feynman diagrams containing the bare Green functions and an increasing number of electron-phonon vertices.
Partial resummation leads to the Dyson equations

$$G(k, i\omega_n)^{-1} = G_0(k, i\omega_n)^{-1} - \Sigma(k, i\omega_n) \tag{18}$$
$$D(q, i\nu_m)^{-1} = G_0(q, i\nu_m)^{-1} - \Pi(q, i\nu_m)\,, \tag{19}$$

which connects bare and renormalized Green functions via the electron and phonon self-energy, Σ and Π, respectively. The self-energies are defined as the sum of all one-particle irreducible Feynman diagrams, i.e., as the sum of all Feynman diagrams, which cannot be separated into two distinct graphs by cutting a single electron or phonon line.
In the following we will discuss the most important contributions to the self-energies in more detail.

3.2 Electron self-energy

The lowest-order diagram of the electron self-energy represents the virtual exchange of a phonon as shown in Fig. 2

$$\Sigma_{ep}(k, i\omega_n) = -\frac{1}{\beta}\sum_{n'}\frac{1}{N_q}\sum_{k',q} g^q_{k',k} G_0(k', i\omega_{n'})(g^q_{k',k})^* D_0(q, i\omega_{n'} - i\omega_n)\,. \tag{20}$$

After performing the Matsubara sum over $\omega_{n'}$ one obtains

$$\Sigma_{ep}(k, i\omega_n) = \frac{1}{N_q}\sum_{k',q} |g^q_{k',k}|^2 \left(\frac{b(\omega_q) + f(\varepsilon_{k'})}{i\omega_n + \omega_q - \varepsilon_{k'}} + \frac{b(\omega_q) + 1 - f(\varepsilon_{k'})}{i\omega_n - \omega_q - \varepsilon_{k'}}\right). \tag{21}$$

Σ_{ep} depends on temperature T via the Fermi and Bose distribution functions, $f(\varepsilon) = (e^{\varepsilon/T} + 1)^{-1}$ and $b(\omega) = (e^{\omega/T} - 1)^{-1}$, respectively.

To discuss the quasiparticle renormalization, we consider the retarded Green function, which is obtained by analytic continuation to the real axis via $i\omega_n \to \varepsilon + i\delta$ with an infinitesimal positive δ. It is connected to the analytic continuation of the self-energy via the Dyson equation

$$G(k,\varepsilon) = (\varepsilon - \varepsilon_k - \Sigma(k,\varepsilon))^{-1}\,. \tag{22}$$

If the self-energy is small enough, the spectral function $A_k(\varepsilon) = -\mathrm{Im}\, G(k, \varepsilon + i\delta)$ consists of a well defined peak at a shifted quasiparticle energy determined by the real part of Σ

$$\overline{\varepsilon}_k = \varepsilon_k + \mathrm{Re}\,\Sigma(k,\overline{\varepsilon}_k)\,. \tag{23}$$

The quasiparticle acquires a finite lifetime leading to a linewidth (full width at half maximum)

$$\Gamma_k = -2\mathrm{Im}\,\Sigma(k,\overline{\varepsilon}_k)\,, \tag{24}$$

which is determined by the imaginary part.
It is straightforward to perform the analytic continuation of $\Sigma_{ep}(k, i\omega_n \to \varepsilon + i\delta)$ in the form given in Eq. (21) and to derive the expression for the imaginary part

$$\begin{aligned}\mathrm{Im}\,\Sigma_{ep}(k,\varepsilon) = -\pi\frac{1}{N_q}\sum_{k',q}|g^q_{k',k}|^2\Big(\quad &\delta(\varepsilon-\varepsilon_{k'}+\omega_q)(b(\omega_q)+\quad f(\varepsilon_{k'}))\\ &+\delta(\varepsilon-\varepsilon_{k'}-\omega_q)(b(\omega_q)+1-f(\varepsilon_{k'}))\Big).\end{aligned} \tag{25}$$

This can be rewritten by introducing two spectral functions

$$\alpha^2F^{\pm}_k(\varepsilon,\omega) = \frac{1}{N_q}\sum_q \delta(\omega-\omega_q)\sum_{k'}|g^q_{k',k}|^2\delta(\varepsilon-\varepsilon_{k'}\pm\omega)\,. \tag{26}$$

They depend on the electronic state k via the EPC vertex. The imaginary part can then be cast in the form

$$\mathrm{Im}\,\Sigma_{ep}(k,\varepsilon) = -\pi\int_0^\infty d\omega\Big(\alpha^2F^+_k(\varepsilon,\omega)[b(\omega)+f(\omega+\varepsilon)]+\alpha^2F^-_k(\varepsilon,\omega)[b(\omega)+f(\omega-\varepsilon)]\Big). \tag{27}$$

The physical interpretation of this expression is as follows. When a quasiparticle hole is created at a state k ($\varepsilon < \varepsilon_F$), electrons can scatter from states with higher or lower energies, respectively (see Fig. 3). By conservation of energy, the first process involves a simultaneous emission of a phonon, while the second one is related to the absorption of a phonon. The probability is described by $\alpha^2F^-_k$ and $\alpha^2F^+_k$, respectively, weighted with the appropriate bosonic and fermionic distribution functions. Both processes provide decay channels contributing additively to the linewidth (inverse lifetime) of the quasiparticle. A similar description holds when a quasiparticle (electron) is created at energies above the Fermi level.
Very often, a simplification is made which is called the quasielastic approximation. Because the electronic energy scale is typically much larger than the phonon energies, differences between emission and absorption spectra are rather small, and it is well justified to ignore the phonon energy ω_q in the δ-function of (26), such that $\alpha^2F^{\pm}_k \approx \alpha^2F_k$ with

$$\alpha^2F_k(\varepsilon,\omega) = \frac{1}{N_q}\sum_q \delta(\omega-\omega_q)\sum_{k'}|g^q_{k',k}|^2\delta(\varepsilon-\varepsilon_{k'})\,. \tag{28}$$

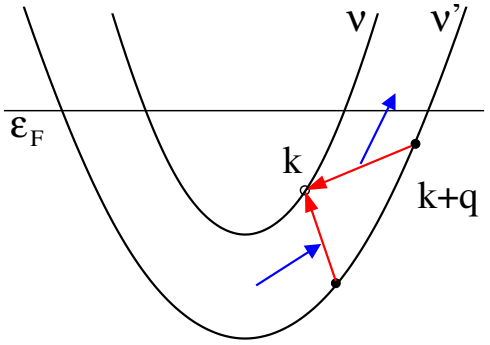

Fig. 3: *Illustration of the scattering processes contributing to the self-energy of a hole quasiparticle with momentum* **k** *and band index* ν*. Electrons (red lines) can scatter virtually from states with higher or lower energies under simultaneous emission or absorption of a phonon (blue lines), respectively.*

The self-energy then simplifies to

$$\mathrm{Im}\,\Sigma_{ep}(k,\varepsilon) = -\pi \int_0^\infty d\omega \Big(\alpha^2 F_k(\varepsilon,\omega)[2b(\omega) + f(\omega+\varepsilon) + f(\omega-\varepsilon)] \Big). \tag{29}$$

It is instructive to evaluate this expression for the simple Einstein model, where only a single dispersionless phonon mode with energy Ω couples to the electrons. In the limit $T \to 0$ one finds

$$\mathrm{Im}\,\Sigma_{ep}(k,\varepsilon) \to -\pi A(\varepsilon)\big(2 - \Theta(\Omega-\varepsilon) - \Theta(\Omega+\varepsilon)\big)\,, \tag{30}$$

where $\Theta(x)$ denotes the Heaviside step function, and $A(\varepsilon) = 1/N_k \sum_{k',q} |g^q_{k',k}|^2 \delta(\varepsilon - \varepsilon_{k'})$ represents the density of states at energy ε weighted by scattering matrix elements. Typically $A(\varepsilon)$ is slowly varying on the scale of phonon energies. On contrast, $\Sigma_{ep}(\varepsilon)$ vanishes for energies $|\varepsilon| < \Omega$ and shows a step at Ω, because of the presence of the step functions. This reflects the fact that no phonon modes are available for decay when $|\varepsilon| < \Omega$. $\mathrm{Re}\,\Sigma_{ep}$ can be obtained via the Kramers-Kronig relation

$$\mathrm{Re}\,\Sigma_{ep}(k,\varepsilon) = \frac{1}{\pi} \int d\varepsilon' \, \frac{\mathrm{Im}\,\Sigma_{ep}(k,\varepsilon')}{\varepsilon - \varepsilon'}\,. \tag{31}$$

As shown in Fig. 4(a) it contains a maximum at $\varepsilon = \Omega$ and has a finite slope at $\varepsilon \to 0$. The resulting dispersion for the renormalized quasiparticle is sketched in Fig. 4(b). It shows two characteristics: (i) the dispersion is strongly modified in the vicinity of ε_F in the range of phonon energies, altering the Fermi velocity related to the slope of $\mathrm{Re}\,\Sigma_{ep}(\varepsilon \to 0)$. (ii) A cusp appears at $\varepsilon = \pm\Omega$.

For a more realistic phonon spectrum which covers continuously an energy range $0 \le \omega \le \omega_{\max}$, the step-like feature in $\mathrm{Im}\,\Sigma_{ep}(\varepsilon)$ is washed out, but $\Sigma_{ep}(\varepsilon)$ still varies rapidly in the energy range of the phonons. The cut in the renormalized dispersion is then replaced by a kink. An example of an experimentally determined self-energy is given in Fig. 4(c) and (d).

The spectral function $\alpha^2 F_k$ contains the essential information related to the electron-phonon coupling of the specific electronic state $k = (\mathbf{k}\nu)$. A convenient measure for the strength of the

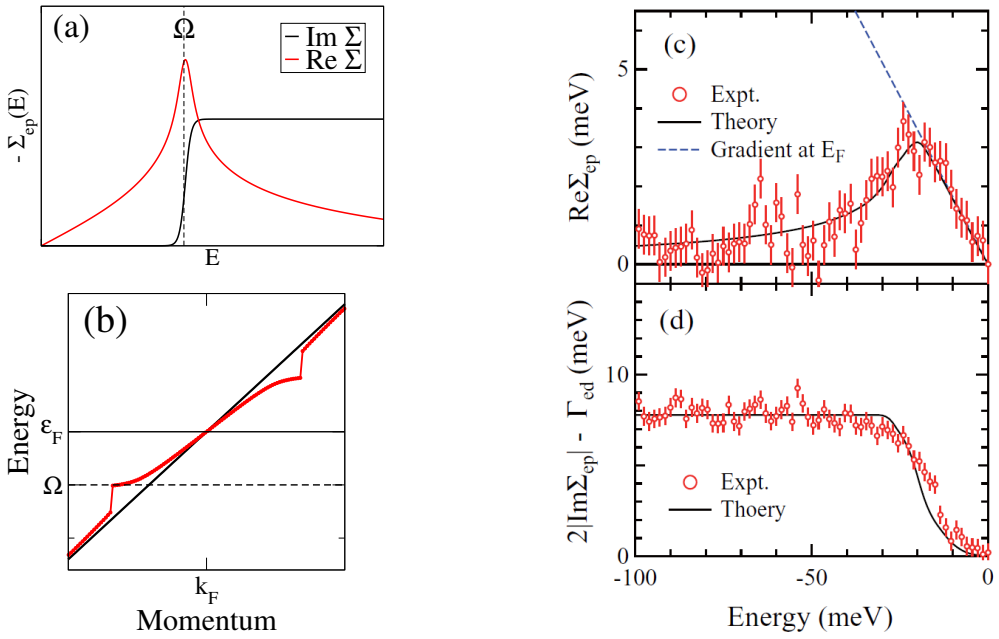

Fig. 4: *Illustration of the renormalization of an electronic band coupling to an Einstein-type phonon branch with energy Ω. (a) Real and imaginary part of the electron self-energy. (b) Renormalized quasiparticle dispersion, showing a kink at the phonon frequency. (c) Real and (d) imaginary part of the electron self-energy extracted from angle-resolved photoemission spectroscopy measurements taken for an electronic surface band of the Cu(110) surface. After Jiang* et al. *[8]*

EPC is the dimensionless coupling parameter

$$\lambda_k = 2 \int d\omega \, \frac{\alpha^2 F_k(\bar{\varepsilon}_k, \omega)}{\omega} \, . \tag{32}$$

It characterizes the strength of the coupling of a specific electronic state to the whole phonon spectrum, and depends both on the momentum and band character of the electronic state.
There are two relations which connect this parameter to experimentally accessible quantities. The first is related to the real part of the self-energy for an electronic band crossing the Fermi level:

$$\lambda_k = \left. \frac{\partial \mathrm{Re}\, \Sigma_{ep}(k, \varepsilon)}{\partial \varepsilon} \right|_{\varepsilon=0, T=0} \, . \tag{33}$$

Thus the coupling constant is given by the slope of $\mathrm{Re}\Sigma_{ep}$ right at the Fermi energy in the limit $T \to 0$. λ_k is also called the mass-enhancement parameter, because the quasiparticle velocity is changed to $v_F^* = v_F/(1+\lambda_k)$ and can be interpreted as an enhanced effective mass $m_k^* = m_k(1+\lambda_k)$, where m_k denotes the unrenormalized mass. Eq. (33) is often utilized in ARPES measurements of bands crossing the Fermi level, which attempt to extract the energy dependence of the real part of the self-energy.
A second route to determine the coupling constant of an electronic state is via the temperature dependence of the linewidth

$$\Gamma_k = \pi \int_0^\infty d\omega \Big(\alpha^2 F_k(\bar{\varepsilon}_k, \omega) [2b(\omega) + f(\omega + \bar{\varepsilon}_k) + f(\omega - \bar{\varepsilon}_k)] \Big) \, . \tag{34}$$

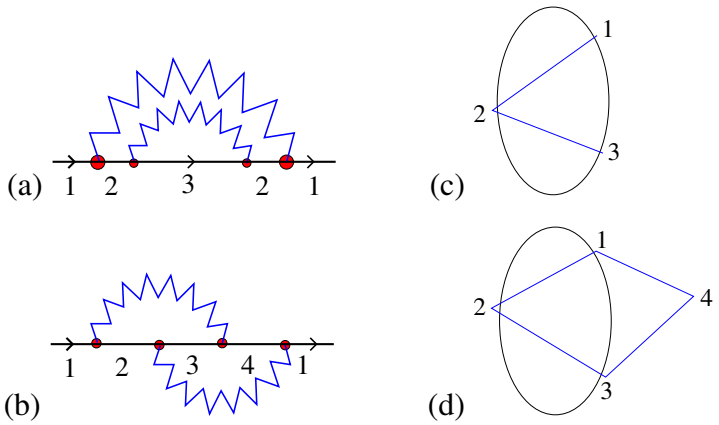

Fig. 5: *(a) and (b) Diagrammatic representation of the two second-order contributions to the electron self-energy. Blue zigzag lines represent phonon and black lines electron propagators. (c) and (d) Schematic drawing of the Fermi surface and the states contributing to the graphs (a) and (b), respectively.*

In Eq. (34), the T-dependence it contained solely in the Bose and Fermi distribution functions. For $T \to 0$, it approaches a finite value given by

$$\Gamma_k \to 2\pi \int_0^{\omega_{\max}} d\omega \, \alpha^2 F_k(\bar{\varepsilon}_k, \omega) \, . \tag{35}$$

With increasing T, the linewidth increases for all energies. For temperatures larger than the maximum phonon frequencies, this T-dependence becomes almost linear, and its slope is determined by the average coupling parameter defined above

$$\Gamma_k \approx 2\pi \lambda_k T \, . \tag{36}$$

This relationship has been widely used to extract λ_k from measurements of $\Gamma_k(T)$, in particular for surface electronic states.

3.3 Migdal's theorem

So far we have discussed the influence of phonons on the electronic properties in lowest order of the electron-phonon coupling. What about higher-order corrections? A very important answer is given by the *Migdal's theorem*, which is relevant for both the normal-state properties discussed here and the Eliashberg theory of superconductivity presented in the next section. We give only a very brief qualitative discussion here, more details can be found in literature [9,10,7]. Fig. 5 (a) and (b) show two next-order corrections to Σ_{ep}. The first is a self-energy contribution to an inner line and can be taken into account by using the full Green function G for the intermediate state instead of G_0. In contrast, the graph in Fig. 5(b) is a *vertex correction*. Migdal's theorem now states that vertex corrections are small compared to self-energy graphs and can be neglected. More precisely, this is true for those parts of the renormalized Green function which are sensitive to the phonons. Such contributions involve intermediate states whose energies are close to each other.

Fig. 6: *(a) Diagrammatic representation of the imaginary part of the phonon self-energy up to second order in the electron-phonon vertex. Blue zigzag lines represent phonon, black lines electron propagators.*

Fig. 5(c) and (d) show schematically the Fermi surfaces and the states which make a contribution to the graphs in Fig. 5(a) and (b), respectively. The first case contains only small energy differences $\varepsilon_{12} = \varepsilon_1 - \varepsilon_2$ and ε_{13}. In the second case, momentum conservation leads to a large difference ε_{14}. This unfavorable situation can only be avoided when one of the intermediate phonon momenta becomes small. Migdal showed, that for normal metals the phase space for such processes is very small, and the contribution from graph Fig. 5(d) is by a factor ω_D/ε_F smaller than that from graph (a), where ω_D denotes the Debye frequency, ε_F the Fermi energy. Thus ω_D/ε_F represents a typical ratio of phononic and electronic energy scales which is of the order of 0.1.

The phase space argument of Migdal's theorem breaks down in two circumstances: (i) For a significant part of processes both phonons have small q (both $k_2 - k_1$ and $k_3 - k_2$ are small). This can happen in metals with very small Fermi surfaces, for example in low-doped semiconductors. (ii) Metals with a one-dimensional Fermi surface topology (quasi-1D). In addition, Migdal's theorem becomes questionable in the case of metals with very small band widths, where the ratio ω_D/ε_F is not small any more.

According to Migdal's theorem, Σ_{ep} is well represented by the single graph shown in Fig. 2, except that G_0 is replaced by G, and other contributions can be neglected. According to arguments given by Migdal and Holstein, this replacement again gives small corrections of the order of ω_D/ε_F [9, 11]. Thus to a good approximation it is justified to use G_0, so the previous formulas still hold. This approximation does not work anymore for the superconducting state, as discussed in the next section.

However, the analysis given above rests on a simplified solution of the Dyson equation which can break down for larger coupling. Then the renormalization becomes much more involved and requires the solution of the Dyson equation in the complex plane [12]. The spectral function develops a complex structure, which indicates the break-down of the quasiparticle picture.

3.4 Phonon self-energy and linewidth

The EPC also renormalizes the phononic quasiparticles. The measurement of the phonon linewidth actually provides another way to gain experimental information about the coupling strength. We will briefly sketch this approach here.

The finite linewidth or inverse lifetime of a phonon mode is connected to the imaginary part of the phonon self-energy by $\gamma_q = -2\mathrm{Im}\Pi_q(\omega)$. The lowest-order diagram contributing to $\Pi_q(\omega)$

is shown in Fig. 6

$$\begin{aligned} \Pi_q(i\nu_m) &= \frac{1}{\beta}\sum_n \frac{1}{N_k}\sum_{k,k'} |g^q_{k',k}|^2 \; G_0(k, i\omega_n)\, G_0(k'\nu', i\omega_n + i\nu_m) \\ &= \frac{1}{N_k}\sum_{k',k} |g^q_{k',k}|^2 \; \frac{f(\varepsilon_k) - f(\varepsilon_{k'})}{i\nu_m + \varepsilon_k - \varepsilon_{k'}}\,, \end{aligned} \tag{37}$$

leading after analytic continuation to the following expression for the linewidth (half-width at half maximum)

$$\gamma_q = -2\mathrm{Im}\Pi_q(\omega_q) = 2\pi\frac{1}{N_k}\sum_{k',k} |g^q_{k',k}|^2 \big(f(\varepsilon_k) - f(\varepsilon_{k'})\big)\delta(\omega_q + (\varepsilon_k - \varepsilon_{k'}))\,. \tag{38}$$

This expression contains the T-dependence via the Fermi distribution functions f. Because phonon energies are typically small compared to electronic energies, the energy difference $\varepsilon_k - \varepsilon_{k'}$ is also small, and one can approximate

$$f(\varepsilon_k) - f(\varepsilon_{k'}) \approx f'(\varepsilon_k)(\varepsilon_k - \varepsilon_{k'}) \to -f'(\varepsilon_k)\omega_q \tag{39}$$

with $f' = df/d\varepsilon$. For $T \to 0$, $f'(\varepsilon_k) \to -\delta(\varepsilon_k)$, and by neglecting ω_q inside the δ-function, the expression further simplifies to

$$\gamma_q = 2\pi\omega_q\frac{1}{N_k}\sum_{k',k} |g^q_{k',k}|^2 \; \delta(\varepsilon_k)\,\delta(\varepsilon_{k'})\,. \tag{40}$$

This approximate expression for the linewidth, first derived by Allen [13], is widely used in numerical calculations. As will be discussed in the next section, γ_q in the form of Eq. (40) enters directly the expression for the coupling strength of a phonon mode relevant for superconductivity. Thus measurements of the phonon linewidths, for example by inelastic neutron or X-ray scattering experiments, provide information about the importance of a phonon mode for the pairing. One has to keep in mind, however, that γ_q only represents the contribution from EPC, while the experimental linewidth also contains other contributions like those from anharmonic decay processes. Furthermore, approximation (40) does not hold in the limit $\mathbf{q} \to 0$ for metals, because the phonon frequency in Eq. (38) cannot be neglected anymore for intraband contributions, which involve arbitrarily small energy differences $\varepsilon_k - \varepsilon_{k'}$.

4 Phonon-mediated superconductivity

Superconductivity is a macroscopic quantum phenomenon of the electron system. Its origin lies in an instability of the Fermi liquid state that leads to a new ground state of correlated paired electrons (Cooper pairs). In their seminal paper, Bardeen, Cooper, and Schrieffer (BCS) [14] have shown that this state is stabilized, whenever there exists an attractive interaction among two electrons. Such an attractive interaction is always provided by the electron-phonon coupling, which thus represents a natural source for pairing in any metal. EPC is known to be the pairing

mechanism in most superconductors, which are commonly termed classical superconductors to distinguish them from more exotic materials where other types of pairing mechanism are suspected.
The BCS theory treated the EPC only in a simplified form appropriate for the weak coupling limit. A more complete theory has been soon after worked out applying many-body techniques (for reviews see, e.g., Refs. [15, 10, 16, 17]) . The resulting Eliashberg theory [18] extends the framework of BCS into the strong coupling regime and allows a quantitative prediction of many properties of the superconducting state. An important property of the superconducting state is that the quasiparticle spectrum is gaped. The size of the gap plays the role of an order parameter. In the following, we discuss the essential ingredients of the theory of strong-coupling phonon-mediated superconductivity, also known as the Migdal-Eliashberg theory. First, we give a simple derivation of an effective electron-electron interaction mediated by phonons. Using many-body techniques we then derive the superconducting gap equations and identify the important quantities related to the electron-phonon coupling, which determine the superconducting properties.

4.1 Effective electron-electron interaction

The coupling of the electrons to the phonon system does introduce an effective electron-electron interaction, which can act as a pairing interaction evoking the superconducting state. The general approach using many-body techniques will be discussed below. Here a simple but instructive derivation of the effective interaction is given with the help of a properly chosen canonical transformation. To simplify the discussion, we will consider the case of a single, spinless quasiparticle band coupled to a single phonon (boson) mode. The Fröhlich Hamiltonian then reads ($g_{\mathbf{k},\mathbf{q}} \equiv g^{\mathbf{q}}_{\mathbf{k}+\mathbf{q},\mathbf{k}}$)

$$H = \sum_{\mathbf{k}} \varepsilon_{\mathbf{k}}\, c^{\dagger}_{\mathbf{k}} c_{\mathbf{k}} + \sum_{\mathbf{q}} \omega_{\mathbf{q}} \left(b^{\dagger}_{\mathbf{q}} b_{\mathbf{q}} + \frac{1}{2} \right) + \sum_{\mathbf{kq}} g_{\mathbf{k},\mathbf{q}}\, c^{\dagger}_{\mathbf{k}+\mathbf{q}} c_{\mathbf{k}} \left(b_{\mathbf{q}} + b^{\dagger}_{-\mathbf{q}} \right) . \tag{41}$$

Let us consider the Hamiltonian

$$H = H_0 + \eta H_1 \,, \tag{42}$$

where H_0 is the unperturbed Hamiltonian, H_1 the perturbation, and η represents an expansion coefficient, which is considered to be small. The idea is to perform a canonical transformation

$$H' = e^{-\eta S} H e^{\eta S} \tag{43}$$

and eliminate the first-order term in η by choosing the operator S appropriately. Expanding Eq. (43) in a power series in η gives

$$H' = H + \eta[H, S] + \frac{\eta^2}{2}[[H, S], S] + O(\eta^3) \tag{44}$$

$$= H_0 + \eta(H_1 + [H_0, S]) + \eta^2[H_1, S] + \frac{\eta^2}{2}[[H_0, S], S] + O(\eta^3) \,. \tag{45}$$

To eliminate the term linear in η one has to find an S which fulfills the condition

$$H_1 + [H_0, S] = 0\,. \tag{46}$$

Then the transformed Hamiltonian can be written as

$$H' = H_0 + H_{\text{eff}} + O(\eta^3) \qquad \text{with} \quad H_{\text{eff}} = \frac{\eta^2}{2}[H_1, S]\,. \tag{47}$$

This general approach is now applied to the Fröhlich Hamiltonian (41) with $H_0 = H_e + H_{ph}$ and $\eta H_1 = H_{e-ph}$. For the canonical operator we make the ansatz

$$S = \sum_{\mathbf{kq}} g_{\mathbf{k},\mathbf{q}}\, c^\dagger_{\mathbf{k}+\mathbf{q}} c_{\mathbf{k}} \left(x_{\mathbf{k},\mathbf{q}} b_{\mathbf{q}} + y_{\mathbf{k},\mathbf{q}} b^\dagger_{-\mathbf{q}} \right)\,. \tag{48}$$

The parameters $x_{\mathbf{k},\mathbf{q}}$ and $y_{\mathbf{k},\mathbf{q}}$ will be determined in order to fulfill Eq. (46). Evaluating the commutators gives

$$[H_e, S] = \sum_{\mathbf{kq}} g_{\mathbf{k},\mathbf{q}}\, (\varepsilon_{\mathbf{k}+\mathbf{q}} - \varepsilon_{\mathbf{k}}) c^\dagger_{\mathbf{k}+\mathbf{q}} c_{\mathbf{k}} \left(x_{\mathbf{k},\mathbf{q}} b_{\mathbf{q}} + y_{\mathbf{k},\mathbf{q}} b^\dagger_{-\mathbf{q}} \right) \tag{49}$$

$$[H_{ph}, S] = \sum_{\mathbf{kq}} g_{\mathbf{k},\mathbf{q}}\, c^\dagger_{\mathbf{k}+\mathbf{q}} c_{\mathbf{k}} \left(-x_{\mathbf{k},\mathbf{q}} \omega_{\mathbf{q}} b_{\mathbf{q}} + y_{\mathbf{k},\mathbf{q}} \omega_{-\mathbf{q}} b^\dagger_{-\mathbf{q}} \right)\,. \tag{50}$$

Using the relation $\omega_{\mathbf{q}} = \omega_{-\mathbf{q}}$ this combines to

$$H_1 + [H_0, S] = \sum_{\mathbf{kq}} g_{\mathbf{k},\mathbf{q}} c^\dagger_{\mathbf{k}+\mathbf{q}} c_{\mathbf{k}} \Big(\quad \big(1 + (\varepsilon_{\mathbf{k}+\mathbf{q}} - \varepsilon_{\mathbf{k}} - \omega_{\mathbf{q}})\, x_{\mathbf{k},\mathbf{q}}\big) b_{\mathbf{q}} \tag{51}$$

$$+ \big(1 + (\varepsilon_{\mathbf{k}+\mathbf{q}} - \varepsilon_{\mathbf{k}} + \omega_{\mathbf{q}})\, y_{\mathbf{k},\mathbf{q}}\big) b^\dagger_{-\mathbf{q}} \Big)\,. \tag{52}$$

This expression vanishes when

$$x_{\mathbf{k},\mathbf{q}} = (\varepsilon_{\mathbf{k}} - \varepsilon_{\mathbf{k}+\mathbf{q}} + \omega_{\mathbf{q}})^{-1} \quad \text{and} \quad y_{\mathbf{k},\mathbf{q}} = (\varepsilon_{\mathbf{k}} - \varepsilon_{\mathbf{k}+\mathbf{q}} - \omega_{\mathbf{q}})^{-1}\,. \tag{53}$$

The last step is to evaluate the effective interaction Eq. (47). The commutator $[H_1, S]$ has the form $[Aa, Bb]$ with $A, B \propto c^\dagger c$ containing products of fermion operators, and $a, b \propto xb + yb^\dagger$ containing sums of boson operators. From the general relationship $[Aa, Bb] = AB[a, b] + [A, B]ab - [A, B][a, b]$ it is easy to see that there are three types of contributions. Keeping in mind that $[A, B]$ is again a product of the form $c^\dagger c$ and $[a, b]$ a c-number, the last term represents a one-body electron operator, which actually can be shown to vanish. The second term describes an effective coupling of an electron to two phonons, also called a non-linear coupling term.
We are interested in the first term, which is proportional to the product of two fermionic creation and two annihilation operators, $c^\dagger c c^\dagger c$, and thus represents an effective electron-electron interaction. Explicitly it has the form

$$H_{\text{eff}} = \frac{\eta^2}{2} \sum_{\mathbf{kk'q}} g_{\mathbf{k},\mathbf{q}}\, g_{\mathbf{k'},-\mathbf{q}}\, (y_{\mathbf{k'},-\mathbf{q}} - x_{\mathbf{k'},-\mathbf{q}})\, c^\dagger_{\mathbf{k}+\mathbf{q}} c_{\mathbf{k}} c^\dagger_{\mathbf{k'}-\mathbf{q}} c_{\mathbf{k'}} \tag{54}$$

$$= \eta^2 \sum_{\mathbf{kk'q}} V_{\text{eff}}(\mathbf{k}, \mathbf{k'}, \mathbf{q})\, c^\dagger_{\mathbf{k}+\mathbf{q}} c_{\mathbf{k}} c^\dagger_{\mathbf{k'}-\mathbf{q}} c_{\mathbf{k'}} \tag{55}$$

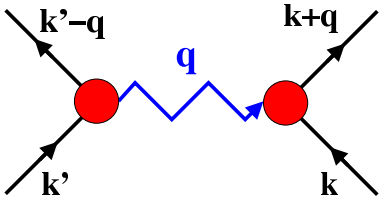

Fig. 7: *Diagrammatic representation of the effective electron-electron interaction mediated by the exchange of a phonon (blue zigzag line). Black lines indicate electronic states.*

with

$$V_{\text{eff}}(\mathbf{k},\mathbf{k}',\mathbf{q}) = g_{\mathbf{k},\mathbf{q}}\, g_{\mathbf{k}',-\mathbf{q}}\, \frac{\omega_{\mathbf{q}}}{(\varepsilon_{\mathbf{k}'} - \varepsilon_{\mathbf{k}'-\mathbf{q}})^2 - \omega_{\mathbf{q}}^2}\,. \tag{56}$$

H_{eff} describes the scattering of two electrons with momenta $\mathbf{k}$ and $\mathbf{k}'$ into states with momenta $\mathbf{k}+\mathbf{q}$ and $\mathbf{k}'-\mathbf{q}$ by the exchange of a virtual boson with momentum $\mathbf{q}$. This process is sketched in Fig. 7.

In the context of pairing in superconductors, the effective interaction between electrons with momenta $\mathbf{k}$ and $-\mathbf{k}$ is of special importance. Using $\varepsilon_{-\mathbf{k}} = \varepsilon_{\mathbf{k}}$ and $g_{-\mathbf{k},-\mathbf{q}} = g^*_{\mathbf{k},\mathbf{q}}$ one obtains

$$V_{\text{eff}}(\mathbf{k},-\mathbf{k},\mathbf{q}) = |g_{\mathbf{k},\mathbf{q}}|^2 \frac{\omega_{\mathbf{q}}}{(\varepsilon_{\mathbf{k}} - \varepsilon_{\mathbf{k}+\mathbf{q}})^2 - \omega_{\mathbf{q}}^2}\,. \tag{57}$$

This effective interaction is attractive (negative) for $|\varepsilon_{\mathbf{k}} - \varepsilon_{\mathbf{k}+\mathbf{q}}| < \omega_{\mathbf{q}}$ and repulsive (positive) for $|\varepsilon_{\mathbf{k}} - \varepsilon_{\mathbf{k}+\mathbf{q}}| > \omega_{\mathbf{q}}$. Eq. (57) shows that the electron-phonon coupling always introduces an attractive interaction for electronic scattering processes involving small energies of the order of phonon energies.

4.2 Nambu formalism

The superconducting state is a macroscopic quantum state, which is characterized by a coherent occupation of Cooper pairs, i.e., states with $(k\uparrow, -k\downarrow)$. In a many-body description, it is related to the appearance of anomalous Green functions

$$F(k,\tau) = -\langle T_\tau c_{k\uparrow}(\tau) c_{-k\downarrow}(0)\rangle \quad F^*(k,\tau) = -\langle T_\tau c^\dagger_{-k\downarrow}(\tau) c^\dagger_{k\uparrow}(0)\rangle \tag{58}$$

originally introduced by Gor'kov [19]. In the normal state these anomalous Green functions vanish. Starting from the Fröhlich Hamiltonian, one can set up a systematic perturbation expansion of the normal and anomalous Green functions, with the goal of obtaining a set of self-consistent equations. A necessary step is a partial resummation of an infinite number of diagrams, because the superconducting state can not be reached in any finite order of the perturbation.

A very convenient way to organize this algebra of diagrams has been introduced by Nambu [20]. One starts by defining the two-component operators

$$\Psi_k = \begin{pmatrix} c_{k\uparrow} \\ c^\dagger_{-k\downarrow} \end{pmatrix} \qquad \Psi^\dagger_k = \begin{pmatrix} c^\dagger_{k\uparrow}, & c_{-k\downarrow} \end{pmatrix} \tag{59}$$

and a 2×2 Green function

$$\underline{G}(k,\tau) = -\langle T_\tau \Psi_k(\tau)\Psi^\dagger_{-k}(0)\rangle = -\begin{pmatrix} \langle T_\tau c_{k\uparrow}(\tau)c^\dagger_{k\uparrow}(0)\rangle & \langle T_\tau c_{k\uparrow}(\tau)c_{-k\downarrow}(0)\rangle \\ \langle T_\tau c^\dagger_{-k\downarrow}(\tau)c^\dagger_{k\uparrow}(0)\rangle & \langle T_\tau c^\dagger_{-k\downarrow}(\tau)c_{-k\downarrow}(0)\rangle \end{pmatrix}$$
$$= \begin{pmatrix} G(k,\tau) & F(k,\tau) \\ F^*(k,\tau) & G(-k,-\tau) \end{pmatrix}. \tag{60}$$

In the following, underlined symbols indicate 2×2 matrices in spin space. Switching to the Fourier transform gives

$$\underline{G}(k,i\omega_n) = \frac{1}{2}\int_{-\beta}^{\beta} d\tau\, e^{i\omega_n\tau}\underline{G}(k,\tau) = \begin{pmatrix} G(k,i\omega_n) & F(k,i\omega_n) \\ F^*(k,i\omega_n) & -G(-k,-i\omega_n) \end{pmatrix}. \tag{61}$$

The next step is to rewrite the Fröhlich Hamiltonian in terms of $\Psi, \Psi^\dagger$. This is most easily done by using the Pauli matrices

$$\underline{\tau}_0 = \begin{pmatrix} 1 & 0 \\ 0 & 1 \end{pmatrix},\ \underline{\tau}_1 = \begin{pmatrix} 0 & 1 \\ 1 & 0 \end{pmatrix},\ \underline{\tau}_2 = \begin{pmatrix} 0 & -i \\ i & 0 \end{pmatrix},\ \underline{\tau}_3 = \begin{pmatrix} 1 & 0 \\ 0 & -1 \end{pmatrix}. \tag{62}$$

The non-interacting electronic part is rewritten as

$$H_e = \sum_{k\sigma} \varepsilon_k\, c^\dagger_{k\sigma}c_{k\sigma} \to \sum_k \varepsilon_k\, \Psi^\dagger_k\, \underline{\tau}_3\, \Psi_k \tag{63}$$

and the interaction part as

$$H_{e-ph} = \sum_{k\sigma}\sum_{\mathbf{q}j} g^q_{k'k}\, c^\dagger_{k'\sigma}c_{k\sigma}\left(b_q + b^\dagger_{-q}\right) \to \sum_k g^q_{k'k}\, \Psi^\dagger_{k'}\, \underline{\tau}_3\, \Psi_k \left(b_q + b^\dagger_{-q}\right). \tag{64}$$

The bare Green function (related to H_e) takes the form

$$\underline{G}_0(k,i\omega_n) = \begin{pmatrix} G_0(k,i\omega_n) & 0 \\ 0 & -G_0(-k,-i\omega_n) \end{pmatrix} = \begin{pmatrix} (i\omega_n - \varepsilon_k)^{-1} & 0 \\ 0 & (i\omega_n + \varepsilon_k)^{-1} \end{pmatrix}$$
$$= \left(i\omega_n\, \underline{\tau}_0 - \varepsilon_k\, \underline{\tau}_3\right)^{-1}. \tag{65}$$

One can show that the Dyson equation retains its usual form

$$\underline{G}^{-1}(k,i\omega_n) = \underline{G}_0^{-1}(k,i\omega_n) - \underline{\Sigma}(k,i\omega_n) \tag{66}$$

with the inversion performed in the 2-dimensional spin space, where the self-energy $\underline{\Sigma}$ is now a 2×2 matrix.

The diagrammatic expansion of the self-energy contains the same diagrams as in the normal state, with the difference that Green functions and vertices are now represented by 2×2 matrices. In particular $g^q_{k'k}$ is replaced by $g^q_{k'k}\,\underline{\tau}_3$.

4.3 Eliashberg theory

The Eliashberg theory is in essence the extension of the normal-state Migdal theory to the superconducting state. Using Migdal's theorem, the only important self-energy diagram is again given by Fig. 2. Within the Nambu formulation this gives

$$\underline{\Sigma}(k,i\omega_n) = -\frac{1}{\beta}\sum_{n'}\frac{1}{N_q}\sum_{k',q} g^q_{k'k}\,\underline{\tau}_3\,\underline{G}(k',i\omega_{n'})\,\underline{\tau}_3\,g^{-q}_{kk'}\,D(q,i\omega_{n'}-i\omega_n)\,. \tag{67}$$

Using the Pauli matrices, $\underline{\Sigma}$ can be written in the general form

$$\underline{\Sigma}(k,i\omega_n) = i\omega_n[1-Z(k,i\omega_n)]\,\underline{\tau}_0 + \chi(k,i\omega_n)\,\underline{\tau}_3 + \Phi(k,i\omega_n)\,\underline{\tau}_1 + \overline{\Phi}(k,i\omega_n)\,\underline{\tau}_2 \tag{68}$$

with as yet unknown and independent real functions Z, χ, Φ, and $\overline{\Phi}$. From the Dyson equation one finds

$$\underline{G}^{-1}(k,i\omega_n) = i\omega_n Z(k,i\omega_n)\,\underline{\tau}_0 - (\varepsilon_k+\chi(k,i\omega_n))\,\underline{\tau}_3 - \Phi(k,i\omega_n)\,\underline{\tau}_1 - \overline{\Phi}(k,i\omega_n)\,\underline{\tau}_2\,. \tag{69}$$

The inverted Green function is then, using $(a_0\underline{\tau}_0+\vec{a}\cdot\vec{\underline{\tau}})(a_0\underline{\tau}_0-\vec{a}\cdot\vec{\underline{\tau}}) = (a_0^2-\vec{a}^2)\underline{\tau}_0$,

$$\underline{G}(k,i\omega_n) = \Big(i\omega_n Z(k,i\omega_n)\,\underline{\tau}_0 + (\varepsilon_k+\chi(k,i\omega_n))\,\underline{\tau}_3 + \Phi(k,i\omega_n)\,\underline{\tau}_1 + \overline{\Phi}(k,i\omega_n)\,\underline{\tau}_2\Big)/\mathcal{D} \tag{70}$$

with $\mathcal{D} := \det\underline{G}^{-1} = (i\omega_n Z)^2 - (\varepsilon_k+\chi)^2 - \Phi^2 - \overline{\Phi}^2$. If one uses this expression for Eq. (67) and separates it into the τ-components, one arrives at four self-consistent equations for the four unknown functions Z, χ, Φ, and $\overline{\Phi}$

$$i\omega_n(1-Z(k,i\omega_n)) = -\frac{1}{\beta}\sum_{n'}\frac{1}{N_q}\sum_{k',q}|g^q_{k'k}|^2 D(q,i\omega_{n'}-i\omega_n)\,\frac{i\omega_{n'}Z(k',i\omega_{n'})}{\mathcal{D}(k',i\omega_{n'})} \tag{71}$$

$$\chi(k,i\omega_n) = -\frac{1}{\beta}\sum_{n'}\frac{1}{N_q}\sum_{k',q}|g^q_{k'k}|^2 D(q,i\omega_{n'}-i\omega_n)\,\frac{\varepsilon_{k'}+\chi(k',i\omega_{n'})}{\mathcal{D}(k',i\omega_{n'})} \tag{72}$$

$$\Phi(k,i\omega_n) = \frac{1}{\beta}\sum_{n'}\frac{1}{N_q}\sum_{k',q}|g^q_{k'k}|^2 D(q,i\omega_{n'}-i\omega_n)\,\frac{\Phi(k',i\omega_{n'})}{\mathcal{D}(k',i\omega_{n'})} \tag{73}$$

$$\overline{\Phi}(k,i\omega_n) = \frac{1}{\beta}\sum_{n'}\frac{1}{N_q}\sum_{k',q}|g^q_{k'k}|^2 D(q,i\omega_{n'}-i\omega_n)\,\frac{\overline{\Phi}(k',i\omega_{n'})}{\mathcal{D}(k',i\omega_{n'})}\,. \tag{74}$$

We note that because momentum conservation determines the phonon momentum, $\mathbf{q} = \mathbf{k}' - \mathbf{k}$, the sum over q is actually only a sum over different phonon branches (j).

Quasiparticle properties are determined by the poles of the Green function after analytic continuation, i.e., from $\mathcal{D}(k,i\omega_n\to\varepsilon+i\delta)=0$. This gives

$$E_k = \sqrt{\frac{(\varepsilon_k+\chi)^2}{Z^2} + \frac{\Phi^2+\overline{\Phi}^2}{Z^2}}\,. \tag{75}$$

The normal state corresponds to a solution $\Phi = \overline{\Phi} = 0$. Z is the quasiparticle renormalization factor, and χ describes shifts in the electron energies. The superconducting state is characterized by a non-zero Φ or $\overline{\Phi}$. From Eq. (75) one can see that the gap function is given by

$$\Delta(k,i\omega_n) = \frac{\Phi(k,i\omega_n) - i\overline{\Phi}(k,i\omega_n)}{Z(k,i\omega_n)} \tag{76}$$

and describes the energy gap in the quasiparticle spectrum. Φ and $\overline{\Phi}$ obey the same equations and are expected have the same functional form up to a common phase factor. This phase factor becomes important in the description of Josephson junctions, but is irrelevant for the thermodynamic properties of a homogeneous superconductor. In the following, we choose the simple gauge $\overline{\Phi} = 0$.

4.4 Isotropic gap equations

The Eliashberg equations (74) represent a complicated non-linear set of equations which couple all momenta k with each other. We will now simplify them and derive the so-called isotropic equations where only the frequency dependence remains. A very detailed derivation was given by Allen and Mitrović [10]. Here we only briefly sketch the main steps. (i) We ignore changes of the phonon quasiparticles and replace D by the unrenormalized Green function

$$D(q, i\nu_m) \to D_0(q, i\nu_m) = \int d\omega \, \delta(\omega - \omega_q) \, \frac{2\omega}{(i\nu_m)^2 - \omega^2} \, . \tag{77}$$

It is then convenient to define the coupling function

$$\alpha^2 F(k, k', \omega) = N(0) \sum_q |g^q_{k'k}|^2 \, \delta(\omega - \omega_q) \, . \tag{78}$$

Again, the sum extends only over the phonon branches j. $N(0) = \frac{1}{N_k} \sum_k \delta(\varepsilon_k)$ denotes the electronic density of states per spin at the Fermi energy. (ii) Similar to the normal state, the electron-phonon self-energy evokes a significant renormalization of quasiparticles only in an energy range $\pm\omega_D$ around the Fermi energy. It is therefore appropriate to consider the quantities Z and ϕ only at the Fermi energy. (iii) We consider only Fermi-surface averages of these quantities. The justification comes from the observation that the superconducting gaps are often very isotropic. Moreover, in real materials, defects are always present which tend to average anisotropic gaps [21]. Under these conditions we can replace the quantities Z and ϕ by their Fermi surface averages, e.g.

$$Z(i\omega_n) = \frac{1}{N_k} \sum_k w_k Z(k, i\omega_n) \tag{79}$$

with weights $w_k = \delta(\varepsilon_k)/N(0)$. Similarly one replaces the coupling function $\alpha^2 F$ by its value at the Fermi surface and averaged over both electron momenta

$$\begin{aligned} \alpha^2 F(\omega) = & \quad \frac{1}{N_k^2} \sum_{kk'} w_k \, w_{k'} \, \alpha^2 F(k, k', \omega) \\ & = \frac{1}{N(0)} \frac{1}{N_k^2} \sum_{kk'} |g^q_{k'k}|^2 \, \delta(\varepsilon_k) \, \delta(\varepsilon_{k'}) \, \delta(\omega - \omega_q) \, , \end{aligned} \tag{80}$$

which defines the *isotropic Eliashberg function*.

The only significant energy dependence comes from $\varepsilon_{k'}$ in the determinant $\mathcal{D}$. Putting everything together gives, for example,

$$\Phi(i\omega_n) = -\frac{1}{\beta}\sum_{n'}\int d\omega\, \frac{2\omega\alpha^2F(\omega)}{(\omega_n-\omega_{n'})^2+\omega^2}\,\Phi(i\omega_{n'})\frac{1}{N_q}\sum_{k'}\,\frac{1}{\mathcal{D}(\varepsilon_{k'},i\omega_{n'})} \tag{81}$$

with $\mathcal{D}(\varepsilon_{k'},i\omega_{n'}) = -[(\omega_{n'}Z(i\omega_{n'})]^2+\Phi(i\omega_{n'})^2+\varepsilon_{k'}^2]$ The final k sum is converted into an integral

$$\frac{1}{N_q}\sum_{k'}\frac{1}{\mathcal{D}(\varepsilon_{k'},i\omega_{n'})} = \int d\varepsilon\, N(\varepsilon)\frac{1}{\mathcal{D}(\varepsilon,i\omega_{n'}))} \approx \frac{-\pi N(0)}{\sqrt{[(\omega_{n'}Z(i\omega_{n'})]^2+\Phi(i\omega_{n'})^2}}\,. \tag{82}$$

In the last step, it was assumed that the electronic density of states $N(\varepsilon)$ does not have a pronounced ε dependence and can be replaced by its value at the Fermi energy. To simplify the following discussion, we will drop the equation for χ thus ignoring the related, often small, shift in the electronic energies. Indeed $\chi = 0$ holds exactly in the limit of infinite band width [17]. Using $\Delta(i\omega_n) = \Phi(i\omega_n)/Z(i\omega_n)$, this finally results in the *isotropic gap equations*

$$\begin{aligned}\omega_n(1-Z(i\omega_n)) &= -\pi\frac{1}{\beta}\sum_{n'}\Lambda(\omega_n-\omega_{n'})\,\frac{\omega_{n'}}{\sqrt{\omega_{n'}^2+\Delta(i\omega_{n'})^2}}\\ \Delta(i\omega_n)Z(i\omega_n) &= \pi\frac{1}{\beta}\sum_{n'}\Lambda(\omega_n-\omega_{n'})\,\frac{\Delta(i\omega_{n'})}{\sqrt{\omega_{n'}^2+\Delta(i\omega_{n'})^2}}\end{aligned} \tag{83}$$

with the interaction kernel

$$\Lambda(\nu_m) = \int d\omega\,\frac{2\omega\alpha^2F(\omega)}{\nu_m^2+\omega^2}\,. \tag{84}$$

The set of non-linear equations (83) must be solved self-consistently for a given temperature T and pairing function α^2F. The kernel entering both equations is an even function of ν_m. It takes its largest value at $\nu_m = 0$

$$\lambda = \Lambda(0) = 2\int d\omega\,\frac{\alpha^2F(\omega)}{\omega}\,. \tag{85}$$

λ is called the (isotropic) coupling constant and is a dimensionless measure of the average strength of the electron-phonon coupling. Depending on its value, materials are characterized as strong ($\lambda > 1$) or weak coupling ($\lambda < 1$) . Due to the factor $1/\omega$ in the integral low-energy modes contribute more to the coupling strength than high-energy modes.

The superconducting state is characterized by a solution with $\Delta(i\omega_n) \neq 0$. The largest T which still allows such a solution defines the critical temperature T_c. Because $\alpha^2F(\omega)$ as defined in Eq. (80) is a positive function, (83) always possess such a superconducting solution for low enough temperatures, i.e., a finite T_c.

An important feature of the Eliashberg gap equations is that they only depend on normal-state properties, which specify a particular material. These comprise the electronic band structure, phonons, and the EPC vertex, quantities which are accessible to *first principles* techniques as discussed in the next section.

At this stage it is useful to make the connection to some normal-state quantities introduced in the previous section. The isotropic Eliashberg function is related to the state-dependent spectral function (28) via appropriate momentum averages at the Fermi energy

$$\alpha^2F(\omega) = \sum_k w_k \alpha^2F_k(\varepsilon = 0, \omega)\,, \tag{86}$$

while the isotropic coupling constant is given by

$$\lambda = \sum_k w_k \lambda_k\,. \tag{87}$$

Similarly, α^2F can be expressed in terms of the phonon linewidths derived in the limit $T \to 0$, Eq. (40), as

$$\alpha^2F(\omega) = \frac{1}{2\pi N(0)} \frac{1}{N_q} \sum_q \frac{\gamma_q}{\omega_q}\, \delta(\omega - \omega_q)\,, \tag{88}$$

which leads to the formula for the isotropic coupling constant

$$\lambda = \frac{1}{\pi N(0)} \frac{1}{N_q} \sum_q \frac{\gamma_q}{\omega_q^2}\,. \tag{89}$$

The dimensionless prefactor γ_q/ω_q in (88) can be interpreted as a measure of the coupling due to an individual phonon mode. The Eliashberg function is then given as a sum over all phonon branches and averaged over phonon momentum.

4.4.1 Coulomb effects

Our derivation up to now was based on the Fröhlich Hamiltonian, where the electronic subsystem is approximated by bands of noninteracting quasiparticles ignoring any Coulomb interaction. The largest consequences of the Coulomb interaction are supposed to be built into the quantities ε_k (and similar into ω_q). The residual Coulomb interaction among the quasiparticles can, however, not be completely neglected in the discussion of phonon-mediated superconductivity. It has a repulsive character and tends to reduce or completely suppress the pairing. The quantity analogous to the electron-phonon coupling constant λ is the Coulomb parameter

$$\mu = N(0) \langle\!\langle V_C(k, k') \rangle\!\rangle_{FS}\,, \tag{90}$$

which is a Fermi surface average of the effective screened Coulomb interaction $V_C(k, k')$. μ is of the order of 1 and thus not a small parameter. But because the electronic timescale is usually much smaller than the vibrational one, or equivalently electronic energies are much larger than phononic ones, only a significantly reduced Coulomb parameter enters the Eliashberg equations. It was shown by Morel and Anderson [22], that the Coulomb repulsion can be taken into account by replacing the kernel in the equation for the gap function by

$$\Lambda(i\omega_n - i\omega_{n'}) \to [\Lambda(i\omega_n - i\omega_{n'}) - \mu^*(\omega_c)]\Theta(\omega_c - |\omega_{n'}|)\,. \tag{91}$$

A cutoff ω_c is introduced which must be chosen to be much larger than phononic energies. The effective Coulomb parameter or *Morel-Anderson Coulomb pseudopotential* obeys a scaling relation

$$\mu^*(\omega_c) = \frac{\mu}{1 + \mu \ln(\varepsilon_0/\omega_c)} \,. \tag{92}$$

ε_0 denotes a characteristic energy scale of the electronic system, where the average matrix elements of the Coulomb interaction becomes small ($\varepsilon_0 \approx$ few ε_F). In practice, μ^* is commonly treated as a phenomenological parameter of the order of ≈ 0.1 for normal metals. A more satisfactory approach, which actually allows to incorporate the Coulomb effects from *first principles*, is the density-functional theory of superconductors [23]. As this is the topic of a separate lecture of this Autumn School, we will not discuss this method further.

4.4.2 Transition temperature T_c

The transition temperature T_c is solely determined by the material-dependent quantities $\alpha^2 F(\omega)$ and μ^*. A thorough numerical analysis of the isotropic gap equations was carried out by Allen and Dynes [24], who used a standard spectrum for $\alpha^2 F$ but varied λ and μ^* over a large parameter range. Their study revealed two important aspects. Firstly, they found that in a reduced parameter space ($\lambda < 2$ and $\mu^* < 0.15$) T_c can be well approximated by a T_c formula proposed originally by McMillan [25], but with a modified prefactor

$$T_c = \frac{\omega_{\log}}{1.2} \exp\left[-\frac{1.04(1+\lambda)}{\lambda - \mu^*(1+0.62\lambda)}\right] . \tag{93}$$

The prefactor contains a properly defined average frequency of the phonon spectrum weighted with the coupling strength

$$\omega_{\log} = \exp\left[\int d\omega \log(\omega) W(\omega)\right] , \tag{94}$$

with the normalized weight function

$$W(\omega) = \frac{2}{\lambda} \frac{\alpha^2 F(\omega)}{\omega} \,. \tag{95}$$

This T_c formula is a significant refinement of the BCS formula $T_c = 1.13\,\omega_D \exp(-1/\lambda)$ derived for the weak-coupling limit.

Secondly, while the T_c formula suggests that T_c approaches a finite value in the limit $\lambda \to \infty$, the isotropic gap equations do not possess a principle upper bound for T_c. Instead the asymptotic relationship

$$T_c \propto \sqrt{\lambda \langle \omega^2 \rangle} \tag{96}$$

holds, where $\langle \omega^2 \rangle$ is the second moment of $W(\omega)$.

5 Density functional theory approach

In the previous sections we have outlined the basic theory for the effects of EPC in the normal and superconducting state. Central quantities are the screened EPC matrix elements, which are not directly accessible from experiment. Thus it is desirable to have a computational scheme which allows materials-dependent predictions. The most common approach is based on density functional theory, which is briefly described in the following.

Density functional theory (DFT) goes back to the seminal works of Hohenberg, Kohn, and Sham [26, 27] and has been outlined in various reviews [28–30]. It provides a framework to map the complex many-body problem of interacting electrons moving in an external potential $v_{\rm ext}(\mathbf{r})$ onto a fictitious system of noninteracting electrons. Their wavefunctions obey a single-particle equation (Kohn-Sham equation) [27]

$$\Big(-\nabla^2 + v_{\rm eff}(\mathbf{r}) \Big) \psi_i(\mathbf{r}) = \varepsilon_i \psi_i(\mathbf{r}) \,. \tag{97}$$

The effective potential $v_{\rm eff}(\mathbf{r})$ is a functional of the density given as the sum of the external potential and a screening potential

$$v_{\rm eff}[n] = v_{\rm ext} + v_{\rm scr}[n] = v_{\rm ext} + v_H[n] + v_{XC}[n] \,. \tag{98}$$

The Hartree and exchange-correlation potentials v_H and v_{XC} are functionals of the density defined as the functional derivative of the Hartree and exchange-correlation energies, $E_H[n] = \int d^3r \int d^3r'\, n(\mathbf{r}) n(\mathbf{r}')/|\mathbf{r}-\mathbf{r}'|$ and E_{XC}. The density is determined by the wavefunctions via

$$n(\mathbf{r}) = \sum_i f_i \, |\psi_i(\mathbf{r})|^2 \,, \tag{99}$$

with f_i the occupation number of the single-particle state ψ_i. Eqs. (97) and (99) have to be solved self-consistently.

An expression for the EPC matrix elements is then derived within a linear-response scheme in the following way. For a solid, $v_{\rm ext}$ represents the sum of ionic potentials felt by the electrons. A small displacement of an atom evokes a perturbation in $v_{\rm ext}$, which translates via the self-consistent equations into a perturbation of $v_{\rm eff}(\mathbf{r})$

$$\begin{aligned} \delta v_{\rm eff}(\mathbf{r}) &= \delta v_{\rm ext}(\mathbf{r}) + \delta v_{\rm scr}(\mathbf{r}) = \delta v_{\rm ext}(\mathbf{r}) + \int d^3r'\, I(\mathbf{r},\mathbf{r}')\, \delta n(\mathbf{r}') \\ I(\mathbf{r},\mathbf{r}') &\equiv \frac{\delta v_{\rm scr}(\mathbf{r})}{\delta n(\mathbf{r}')} = \frac{\delta v_{\rm H}(\mathbf{r})}{\delta n(\mathbf{r}')} + \frac{\delta v_{\rm XC}(\mathbf{r})}{\delta n(\mathbf{r}')} = \frac{2}{|\mathbf{r}-\mathbf{r}'|} + \frac{\delta^2 E_{XC}}{\delta n(\mathbf{r}) \delta n(\mathbf{r}')} \,. \end{aligned} \tag{100}$$

In first-order perturbation theory the variation of the single-particle wavefunctions is

$$\delta\psi_i(\mathbf{r}) = \sum_{j(\neq i)} \frac{\langle j|\delta v_{\rm eff}|i\rangle}{\varepsilon_i - \varepsilon_j} \, \psi_j(\mathbf{r}) \,. \tag{101}$$

Using a similar expression for $\delta\psi_i^*(\mathbf{r})$ gives

$$\delta n(\mathbf{r}) = \sum_{i\neq j} \frac{f_i - f_j}{\varepsilon_i - \varepsilon_j} \, \langle j|\delta v_{\rm eff}|i\rangle \, \psi_i^*(\mathbf{r}) \psi_j(\mathbf{r}) \,. \tag{102}$$

Eqs. (100) and (102) must be solved self-consistently. The results are the first-order variation of the density and the effective potential. The latter is then used for a calculation of the EPC matrix elements for a periodic crystal in the following way. One considers a periodic displacement of the ions from their equilibrium positions, $\mathbf{R}_{ls} = \mathbf{R}^0_{ls} + \mathbf{u}_{ls}$ of the form

$$u_{ls\alpha} = U^{\mathbf{q}}_{s\alpha} e^{i\mathbf{q}\mathbf{R}^0_{ls}} + (U^{\mathbf{q}}_{s\alpha})^* e^{-i\mathbf{q}\mathbf{R}^0_{ls}} , \tag{103}$$

where l denotes the unit cell, s specifies the ion inside a unit cell, and α indicates Cartesian coordinates. The wavevector $\mathbf{q}$ determines the periodicity. Applying the self-consistent procedure described above results in the linear response of the effective potential $\frac{\partial v_{\text{eff}}(\mathbf{r})}{\partial U^{\mathbf{q}}_{s\alpha}}$ which is then used to calculate the electron-phonon matrix elements

$$g^{\mathbf{q}j}_{\mathbf{k}+\mathbf{q}\nu',\mathbf{k}\nu} = \sum_{s\alpha} A^{\mathbf{q}j}_{s\alpha} \left\langle \mathbf{k}+\mathbf{q}\nu' \left| \frac{\partial v_{\text{eff}}}{\partial U^{\mathbf{q}}_{s\alpha}} \right| \mathbf{k}\nu \right\rangle . \tag{104}$$

where again the transformation to the normal mode representation was performed (see Eq. (7)). The self-consistency procedure automatically takes into account the important screening effects. Eq. (104) thus enables to calculate the screened EPC matrix elements on a microscopic level, including their full momentum dependence and to resolve the contributions from different electronic bands and phononic modes.

The same perturbational approach can also be used to calculate the harmonic phonon spectrum without further approximations. This approach has been widely used to predict lattice dynamical and EPC properties from *first principles* for a large variety of materials, and has proven to be quite accurate in predicting the pairing strength in phonon-mediated superconductors.

We illustrate this *first principles* approach for two examples of superconductors with remarkable properties, the high-pressure superconductor H_3S and the multiband superconductor MgB_2.

The current record holder with the highest superconducting transition temperature is hydrogen sulfide with a T_c of 203 K [31]. This superconducting phase was reached by applying a huge pressure of more than 200 GPa to a nominally H_2S sample. It was soon recognized that the superconducting phase is actually a high-pressure modification of H_3S. Most remarkably, the experimental discovery was preceded by theoretical predictions of such high T_c based on the Eliashberg theory [32, 33]. DFT studies suggest that the high-pressure phase has a very simple cubic lattice structure which might be slightly distorted into a rhombohedral structure at lower pressures due to small shifts of the H atoms (see upper left panel in Fig. 8). Its electronic structure is characterized by strong covalent H–S bonds which support huge coupling constants of $\lambda \approx 2$, carried predominantly by the high-energy hydrogen vibrations. Therefore, also the effective phonon frequency $\omega_{\log}$ is large, which in conjunction with a large λ leads to the high T_c values. Fig. 8 shows the results of such a calculation for various pressures. Because a large part of the coupling is carried by hydrogen, a large isotope shift of T_c is expected when replacing hydrogen by deuterium. Because of the light mass of hydrogen, anharmonicity likely is important and may change some aspects of these predictions [34]. Nevertheless, these theoretical studies lend strong support to the view that H_3S is a phonon-mediated superconductor.

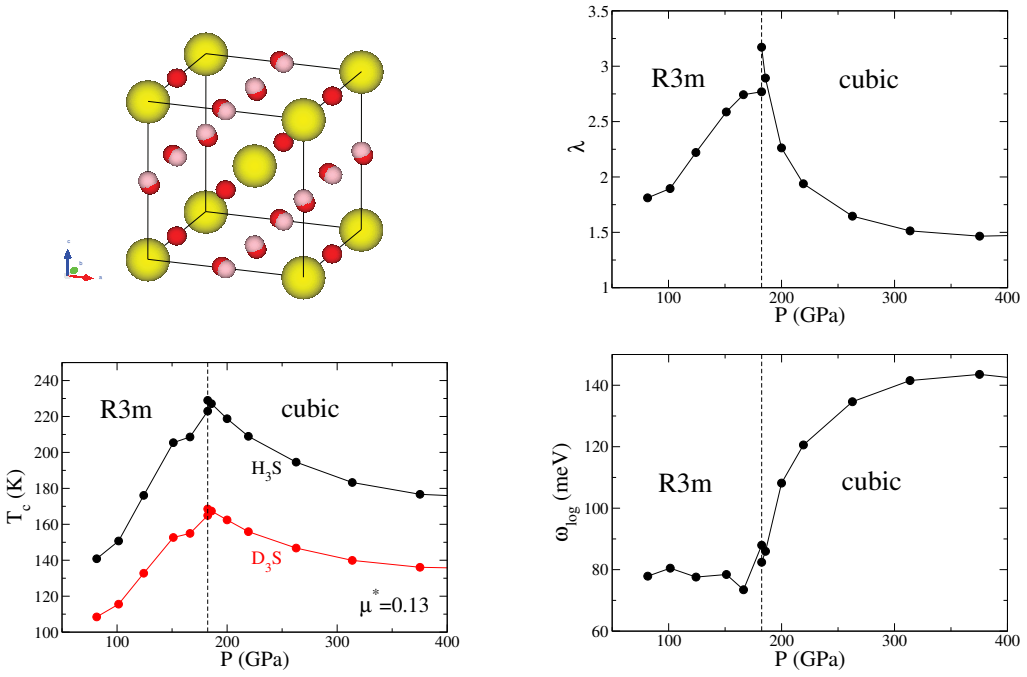

Fig. 8: *Upper left panel: predicted cubic structure of H_3S at high pressures. Large spheres denote S atoms, and small ones H atoms. The red circles indicate the small displacements of H atoms from their ideal cubic positions in the rhombohedral structure predicted for lower pressures. Right panels: variation of λ and $\omega_{\log}$ as function of pressure, respectively. Lower left panel: predicted T_c as calculated from the isotropic gap equations (with μ^* =0.13) as function of pressure. A large isotope shift is expected when replacing hydrogen with deuterium.*

In the previous section, we have restricted our discussion to the isotropic case. Anisotropic superconducting states can be handled using the full momentum dependence of the Eliashberg function (78). This has been done rarely in the past, as the fully anisotropic gap equations are difficult to solve. A special class of anisotropic superconductors are multiband superconductors, which possess several Fermi surface sheets. The superconducting gap can vary among the different sheets, but is approximately isotropic on a single sheet. In this case a partially averaged pairing function is appropriate

$$\alpha^2 F_{\nu\nu'}(\omega) = \frac{1}{N_{\nu'}(0)} \frac{1}{N_q} \sum_{\mathbf{q}j,\mathbf{k}} |g^{\mathbf{q}j}_{\mathbf{k}+\mathbf{q}\nu',\mathbf{k}\nu}|^2 \, \delta(\omega - \omega_{\mathbf{q}j}) \, \delta(\varepsilon_{\mathbf{k}\nu}) \, \delta(\varepsilon_{\mathbf{k}+\mathbf{q}\nu'}) \, . \tag{105}$$

The isotropic Eliashberg function is replaced by a matrix describing intraband and interband pairing contributions.

A textbook example of such a multiband superconductor is MgB_2. Here two types of electronic states are present at the Fermi level, σ and π states, which are derived mainly from the boron p states. Calculations of the band-resolved Eliashberg functions shown in Fig. 9 revealed that the pairing interaction is predominantly driven by the intraband σ–σ contribution. It originates from a strong coupling of σ states to in-plane B vibrations. This peculiar pairing interaction leads to a superconducting state with gaps of different magnitude for the σ and π Fermi surfaces,

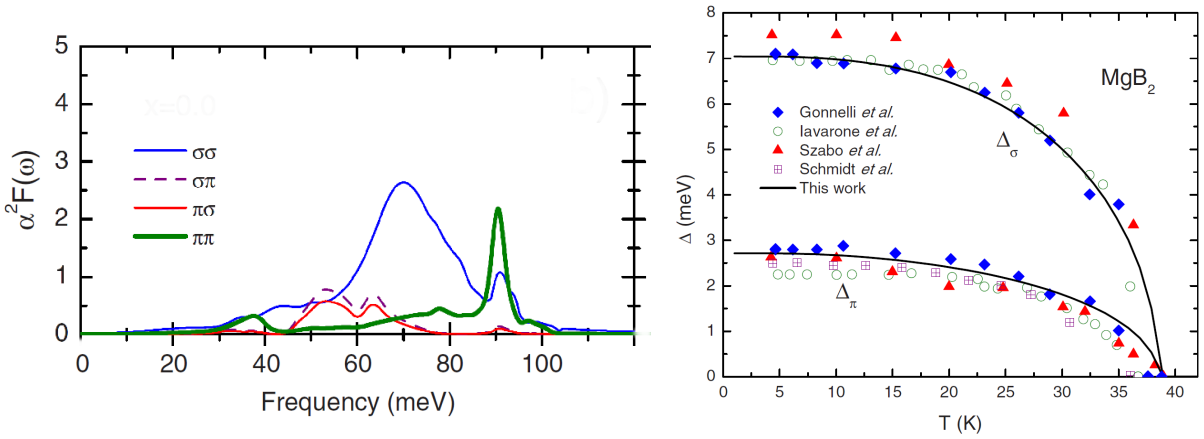

Fig. 9: *Left panel: Calculated band-resolved Eliashberg function for MgB_2. The dominant coupling originates from a large intraband σ–σ pairing interaction. Right panel: Calculated gaps of the σ and π Fermi surfaces as function of temperature. The large gap resides on the σ sheet. Symbols refer to experimental data [35–38]. Figures after [39].*

whose signature could be found, e.g., in specific heat measurements. Combination of *first principles* calculations and a two-band version of the Eliashberg equations were consistent with the experimental T_c of 39 K and could reproduce the measured temperature variation of the two gaps rather well (right panel of Fig. 9).

6 Summary

In this tutorial, an introduction to the theory of the electron-phonon interaction in metals was given. Focus was put on the renormalization properties of electronic and vibronic quasiparticles in the normal state, and on their role for the pairing interaction relevant for the superconducting state. This strong-coupling or Eliashberg theory has been tremendously successful in predicting material-dependent properties of various superconductors in great detail. Density functional theory provides a rather accurate *first principles* computational scheme to calculate the relevant electron-phonon vertex, which is one of the central quantities determining physical observables like electron renormalization, phonon linewidth, or phonon-mediated pairing interaction. Yet one has to keep in mind that the Eliashberg theory incorporates a variety of approximations. The current theoretical challenge is to extend its framework to include the usually neglected aspects of anharmonicity [40], and to quantify electron-phonon coupling effects in materials which are characterized by small electronic energy scales [41] and/or strong electron correlations [42].

Appendices

A Phonon quantization

Within the adiabatic approximation, statics and dynamics of the ions are governed by an effective potential

$$\Omega(\underline{\mathbf{R}}) = V_{ii}(\underline{\mathbf{R}}) + E_0(\underline{\mathbf{R}})\,, \tag{106}$$

where $E_0(\underline{\mathbf{R}})$ denotes the electronic ground-state energy for a given ion configuration $\underline{\mathbf{R}}$. The effective potential Ω builds the starting point of the microscopic theory of lattice dynamics, which has been outlined in a number of review articles [43–45].
Dynamical properties are derived by a systematic expansion of Ω for atom displacements $\mathbf{u}$ around a chosen reference configuration, $\mathbf{R}_i = \mathbf{R}_i^0 + \mathbf{u}_i$, leading to

$$\Omega(\underline{\mathbf{R}}) = \Omega(\underline{\mathbf{R}}^0) + \sum_{i\alpha} \Phi_a(i) u_{i\alpha} + \frac{1}{2} \sum_{i\alpha j\beta} \Phi_{\alpha\beta}(i,j) u_{i\alpha} u_{j\beta} + \dots\,. \tag{107}$$

Greek indices α and β denote Cartesian coordinates, while i and j are atom indices. The term of first order is the negative of the force acting on an atom in the reference configuration

$$F_{i\alpha} = -\left.\frac{\partial \Omega}{\partial R_{i\alpha}}\right|_0 = -\Phi_\alpha(i)\,. \tag{108}$$

It vanishes if one chooses as reference the equilibrium configuration, which minimizes Ω. The second-order coefficients are given by

$$\Phi_{\alpha\beta}(i,j) = \left.\frac{\partial^2 \Omega}{\partial R_{i\alpha} \partial R_{j\beta}}\right|_0 . \tag{109}$$

In periodic crystals, the atoms are characterized by two indices $i = (ls)$, which denote the unit cell (l) and the atoms inside a unit cell (s), respectively. For periodic boundary conditions, the Fourier transform of the force constant matrix is related to the dynamical matrix

$$D_{s\alpha s'\beta}(\mathbf{q}) = \frac{1}{\sqrt{M_s M_{s'}}} \sum_l \Phi_{\alpha\beta}(ls, 0s') e^{-i\mathbf{q}(\mathbf{R}^0_{ls} - \mathbf{R}^0_{0s'})}\,, \tag{110}$$

which determines the equation for the normal modes or phonons,

$$\sum_{s'\beta} D_{s\alpha s'\beta}(\mathbf{q}) \eta_{s'\beta}(\mathbf{q}j) = \omega^2_{\mathbf{q}j} \eta_{s\alpha}(\mathbf{q}j)\,. \tag{111}$$

$\omega_{\mathbf{q}j}$ and $\eta_{s\alpha}(\mathbf{q}j)$ denote the energy and polarization of the normal mode determined by the wavevector $\mathbf{q}$ and branch index j.
These quantities enter into the relationship between the atom displacements and the usual phonon annihilation and creation operators, $b_{\mathbf{q}j}$ and $b^\dagger_{\mathbf{q}j}$, describing quantized normal modes, as given in Eq. (7).

References

[1] G. Grimvall: *The Electron–Phonon Interaction in Metals*, Selected Topics in Solid State Physics, ed. by E. Wohlfarth (North-Holland, New York, 1981)

[2] M. Born and J.R. Oppenheimer, Ann. Physik **84**, 457 (1927)

[3] G.V. Chester and A. Houghton, Proc. Phys. Soc. **73**, 609 (1959)

[4] S.K. Sinha, Phys. Rev. **169**, 477 (1968)

[5] A.A. Abrikosov, L.P. Gorkov, and I.E. Dzyaloshinski: *Methods of Quantum Field Theory in Statistical Physics* (Prentice-Hall, New Jersey, 1964)

[6] A.L. Fetter and J.D. Walecka: *Quantum Theory of Many-Particle Systems* (McGraw-Hill, San Francisco, 1971)

[7] G.D. Mahan: *Many-Particle Physics* (Plenum Press, New York, 1990)

[8] J. Jiang, S.S. Tsirkin, K. Shimada, H. Iwasawa, M. Arita, H. Anzai, H. Namatame, M. Taniguchi, I.Yu. Sklyadneva, R. Heid, K.-P. Bohnen, P.M. Echenique, and E.V. Chulkov, Phys. Rev. B **89**, 085404 (2014)

[9] A.B. Migdal, Sov. Phys. JETP **34**, 996 (1958)

[10] P.B. Allen and B. Mitrović, Solid State Physics **37**, 1 (1982)

[11] T. Holstein, Ann. Phys. **29**, 410 (1964)

[12] A. Eiguren, C. Ambrosch-Draxl, and P.M. Echenique, Phys. Rev. B **79**, 245103 (2009)

[13] P.B. Allen, Phys. Rev. B **6**, 2577 (1972)

[14] J. Bardeen, L.N. Cooper, and J.R. Schrieffer, Phys. Rev. **108**, 1175 (1957)

[15] D.J. Scalapino in R.D. Parks (ed.): *Superconductivity, Vol. 1* (Dekker, New York, 1969)

[16] J.P. Carbotte, Rev. Mod. Phys. **62**, 1027 (1990)

[17] J.P. Carbotte and F. Marsiglio: *Electron-Phonon Superconductivity* in K.H. Bennemann and J.B. Ketterson (eds.): *The Physics of Superconductors* (Springer, 2003)

[18] G.M. Eliashberg, Zh. Eksp. Fiz. **38**, 966 (1960); [Sov. Phys. JETP **11**, 696 (1960)]

[19] L.P. Gor'kov, Zh. Eksp. Teor. Fiz. **34** (1958) [Sov. Phys. JETP **7**, 505 (1958)]

[20] Y. Nambu, Phys. Rev. **117**, 648 (1960)

[21] P.W. Anderson, J. Phys. Chem. Solids **11**, 26 (1959)

[22] P. Morel and P.W. Anderson, Phys. Rev. **125**, 1263 (1962)

[23] L.N. Oliveira, E.K.U. Gross, and W. Kohn, Phys. Rev. Lett. **50**, 2430 (1988)

[24] P.B. Allen and R.C. Dynes, Phys. Rev. B**12**, 905 (1975)

[25] W.L. McMillan, Phys. Rev. **176**, 331 (1968)

[26] P. Hohenberg and W. Kohn, Phys. Rev. B**136**, 864 (1964)

[27] W. Kohn and L.J. Sham, Phys. Rev. A**140**, 1133 (1965)

[28] R.M. Dreizler and E.K.U. Gross:
Density Functional Theory: An Approach to the Quantum Many-Body Problem
(Springer-Verlag, Berlin, 1990)

[29] R.O. Jones and O. Gunnarsson, Rev. Mod. Phys. **61**, 689 (1989)

[30] R.G. Parr and W. Yang: *Density-Functional Theory of Atoms and Molecules*
(Oxford University Press, New York, 1989)

[31] A.P. Drozdov, M.I. Eremets, I.A. Troyan, V. Ksenofontov, and S.I. Shylin,
Nature **525**, 73 (2015)

[32] Y. Li, J, Hao, H. Liu, Y. Li, and Y. Ma, J. Chem. Phys. **140**, 174712 (2014)

[33] D. Duan, Y. Liu, F. Tian, Da Li, X. Huang, Z. Zhao, H. Yu, B. Liu, W. Tian, and T. Cui,
Sci. Rep. **4**, 6968 (2014)

[34] I. Errea, M. Calandra, C.J. Pickard, J.R. Nelson, R.J. Needs, Y. Li, H. Liu, Y. Zhang,
Y. Ma, and F. Mauri, Nature **532**, 81 (2016)

[35] R.S. Gonnelli, D. Daghero, G.A. Ummarino, V.A. Stepanov, J. Jun, S.M. Kazakov, and
J. Karpinski, Phys. Rev. Lett. **89**, 247004 (2002)

[36] M. Iavarone, G. Karapetrov, A.E. Koshelev, W.K. Kwok, G.W. Crabtree, D.G. Hinks,
W.N. Kang, E.M. Choi, H.J. Kim, H.J. Kim, and S.I. Lee,
Phys. Rev. Lett. **89**, 187002 (2002)

[37] P. Szabó, P. Samuely, J. Kačmarčík, T. Klein, J. Marcus, D. Fruchart, S. Miraglia,
C. Marcenat, and A.G.M. Jansen, Phys. Rev. Lett. **87**, 137005 (2001)

[38] H. Schmidt, J.F. Zasadzinski, K.E. Gray, and D.G. Hinks,
Phys. Rev. Lett. **88**, 127002 (2002)

[39] O. de la Peña Seaman, R. de Coss, R. Heid, K.-P. Bohnen, Phys. Rev. B **82**, 224508 (2010)

[40] I. Errea, M. Calandra, and F. Mauri, Phys. Rev. Lett. **111**, 177002 (2013)

[41] L.P. Gor'kov. Phys. Rev. B **93**, 054517 (2016)

[42] Z.P. Yin, A. Kutepov, and G. Kotliar, Phys. Rev. X**3**, 021011 (2013)

[43] M. Born and K. Huang: *Dynamical Theory of Crystal Lattices* (Clarendon Press, Oxford, 1954)

[44] A.A. Maradudin, E.W. Montroll, G.H. Weiss, and I.P. Ipatova: *Solid State Physics, Supplement 3* (Academic Press, New York, 1971), p. 1

[45] H. Boettger: *Principles of the Theory of Lattice Dynamics* (Physik Verlag, Weinheim, 1983)